

Article

Not peer-reviewed version

Non-thermal Plasma Reduces HSV-1 Infection of and Replication in HaCaT Keratinocytes In Vitro

Julia Sutter , Jascha Brettschneider , [Brian Wigdahl](#) , [Peter J. Bruggeman](#) , [Fred Krebs](#) , [Vandana Miller](#) *

Posted Date: 12 January 2024

doi: 10.20944/preprints202401.0962.v1

Keywords: Non-thermal plasma cold atmospheric plasma; low temperature plasma; antiviral; HSV-1 latency; herpes labialis; HSV-1 reactivation; dielectric barrier discharge; cold sore; reactive oxygen and nitrogen species



Preprints.org is a free multidiscipline platform providing preprint service that is dedicated to making early versions of research outputs permanently available and citable. Preprints posted at Preprints.org appear in Web of Science, Crossref, Google Scholar, Scilit, Europe PMC.

Copyright: This is an open access article distributed under the Creative Commons Attribution License which permits unrestricted use, distribution, and reproduction in any medium, provided the original work is properly cited.

Article

Non-Thermal Plasma Reduces HSV-1 Infection of and Replication in HaCaT Keratinocytes *In Vitro*

Julia Sutter ¹, Jascha Brettschneider ¹, Brian Wigdahl ^{1,2}, Peter J. Bruggeman ³, Fred C. Krebs ¹ and Vandana Miller ^{1,*}

¹ Center for Molecular Virology and Gene Therapy, Institute for Molecular Medicine and Infectious Disease, and Department of Microbiology and Immunology, Drexel University College of Medicine, Philadelphia, Pennsylvania, United States of America.

² Sidney Kimmel Cancer Center, Thomas Jefferson University, Philadelphia, Pennsylvania, United States of America.

³ Department of Mechanical Engineering, University of Minnesota, Minneapolis, Minnesota, United States of America.

* Correspondence: vam54@drexel.edu

Abstract: Herpes simplex virus type 1 (HSV-1) is a lifelong pathogen characterized by asymptomatic latent infection in the trigeminal ganglia (TG) with periodic outbreaks of cold sores caused by virus reactivation in the TG and subsequent replication in the oral mucosa. While antiviral therapies can provide relief from cold sores, they are unable to eliminate HSV-1. We provide experimental results that highlight non-thermal plasma (NTP) as a new alternative therapy for HSV-1 infection that would resolve cold sores faster and reduce the establishment of latent infection in the TG. Additionally, this study is the first to explore the use of NTP as a therapy that can both treat and prevent human viral infections. We investigated the antiviral effect of NTP using an in vitro model for HSV-1 cold sores, involving the application of NTP from two separate devices to cell-free HSV-1, HSV-1-infected cells, and uninfected cells. We found NTP reduced the infectivity of cell-free HSV-1, reduced viral replication in HSV-1-infected cells, and diminished the susceptibility of uninfected cells to HSV-1 infection. This triad of antiviral mechanisms of action suggest the potential of NTP as a therapeutic agent effective against HSV-1 infection.

Keywords: Non-thermal plasma cold atmospheric plasma; low temperature plasma; antiviral; HSV-1 latency; herpes labialis; HSV-1 reactivation; dielectric barrier discharge; cold sore; reactive oxygen and nitrogen species

1. Introduction

Herpes simplex virus type 1 (HSV-1) is the causative agent of herpes labialis, an oral infection characterized by the appearance of cold sore lesions. Cold sores are consequences of lytic infection when HSV-1 is actively replicating and producing infectious viruses in mucosal epithelial cells [1,2]. HSV-1 produced by mucosal epithelial cells can also infect sensory neurons in the trigeminal ganglia (TG), resulting in a latent infection. Latency is characterized by a substantial restriction in the number and abundance of viral transcripts as viral replication and virus production are shut down, resulting in an asymptomatic infection in patients. HSV-1 can persist in this latent state for extended periods of time until stress stimuli reactivate lytic infection, causing the re-appearance of clinical symptoms [3,4]. Currently, ~70% of the world's population under the age of 50 harbors an infection with HSV-1 [5]. While the infection is typically mild, its access to the nervous system can allow the spread to nearby organs, causing encephalitis in the brain [6], keratitis in the eye [7], and possibly progressive neurodegenerative disorders like Alzheimer's Disease [8–10]. The risk of developing serious neurodegenerative diseases associated with HSV-1 infection is significant in both immunocompetent and immunocompromised individuals [6,9].

Nucleoside analogs like acyclovir inhibit viral replication in mucosal epithelial cells and are the standard-of-care drugs for treatment of acute HSV-1 infection to alleviate clinical symptoms [11]. However, these antiviral therapies are ineffective in preventing establishment of viral latency in the TG or clearing existing latent reservoirs in sensory neurons. Therefore, HSV-1 continues to persist in the host for the duration of their life with periodic outbreaks of cold sores [12,13]. Due to these

limitations and the ongoing emergence of drug resistant strains of HSV-1 [14], there is a critical need for new therapies that target both the lytic and latent phases of HSV-1 infection in patients. Based on the results of our investigations presented here, we propose that non-thermal plasma (NTP) can address this need.

Plasma medicine is a rapidly developing field that encompasses the biomedical use of NTP for treatment of diseases. NTP is partially ionized gas producing (vacuum) ultraviolet radiation, heat, electric fields, and chemically reactive components, including many reactive oxygen and nitrogen species (RONS) [15]. Pertinent to this study, antiviral activity of NTP has been demonstrated against many viruses with RONS proposed as the dominant effectors [16]. RONS are reactive and can modify structural macromolecular components of the viral particle, as demonstrated in a study where NTP modified the protein capsid of cell-free feline calicivirus (FCV) [17] and reduced virus infectivity [18]. There is also evidence of NTP-generated RONS directly modifying viral components in other human viruses, including hepatitis B virus (HBV) [19], human immunodeficiency virus type 1 (HIV-1) [20], and SARS-CoV-2 [21]. Modifications of virus components may contribute to the reduced infectivity of these viruses.

Thus far, most studies of NTP against cell-free viruses have been focused on the use of NTP as a disinfection agent. While important, most of these investigations have neglected to examine the therapeutic potential of NTP against human infections by viruses like HSV-1. A study in 2014 used explanted corneal cells infected with HSV-1 as an in vitro model for herpes keratitis, and showed that indirect application of NTP resulted in 80% reduction in HSV-1-infected cells with very little cell cytotoxicity [22]. The antiviral effect of NTP against HSV-1 was suggested to correlate with an increase in 8-oxodeoxyguanosine (8-OHdg), a marker of oxidative damage to DNA in infected corneal cells [23]. Neither study tested the therapeutic and clinical potential of NTP as a treatment for cold sores in patients living with HSV-1.

This is the first report of investigations into the treatment and prevention of HSV-1 infection through the direct application of NTP in an in vitro model for HSV-1 cold sores. We hypothesized that the effects of NTP will include (i) reduced virus replication during lytic HSV-1 infection, (ii) reduced infectivity of extracellular HSV-1, and (iii) reduced susceptibility of uninfected cells to infection that would otherwise serve to propagate the spread of HSV-1. To test this hypothesis, our in vitro model for treating cold sores included the direct application of NTP to cell-free HSV-1, HSV-1-infected cells, and uninfected cells. For all experiments, the KOS-GFP-HSV-1 strain, which includes a green fluorescent protein (GFP) reporter replacing a viral immediate-early (IE) gene, was used to quantify HSV-1-infected cells through GFP expression as an indicator of IE viral gene expression [24]. To examine the contributions of RONS as antiviral effectors, we used two devices - a two-dimensional (2D)-DBD device, which delivers large concentrations of RONS to targets and has a demonstrated antiviral effect against different viruses [18] and a floating electrode dielectric barrier discharge (FE-DBD) device, which delivers its biological effects through effectors that include short- and long-lived RONS and electromagnetic fields associated with plasma generation [25]. In cells, RONS are naturally generated by organelles during metabolism, signaling, and immune responses, and neutralized by antioxidants to maintain cellular redox homeostasis. During HSV-1 infection, the virus destabilizes the redox homeostasis by hijacking cellular oxidative stress pathways to craft an environment favorable for their replication and to mitigate immune clearance. NTP-generated RONS can shift the redox environment back in favor of the cell, counteracting viral evasion strategies and potentially promoting HSV-1 clearance [26].

Our studies demonstrated the antiviral effect of direct NTP application on cell-free HSV-1 using two different devices, which were characterized based on their production of long-lived RONS. In addition, NTP reduced viral replication in HSV-1-infected cells and the susceptibility of uninfected cells to HSV-1 infection.

2. Materials and Methods

2.1. HaCaT cell culture

HaCaT adult human keratinocytes [27] were cultured in Dulbecco's Modified Eagle Medium supplemented with 10% fetal bovine serum (FBS), 2 mM L-glutamine, and 1% penicillin/streptomycin (DMEM10). Cells were maintained at 37°C, 5% carbon dioxide (CO₂) at 95% relative humidity and passaged every 3-4 days.

2.2. HSV-1 infection

The KOS-GFP-HSV-1 strain (Figure 1A), which contains a GFP marker in place of the ICP4 gene under the control of a cytomegalovirus (CMV) promoter [24], was prepared at a stock concentration of 3×10^7 PFU/mL. Viral inocula were prepared with serum-free DMEM at multiplicities of infection (MOI; number of viral particles per cell) of 0.1, 0.5, and 1.0 relative to cell numbers plated in each well. HaCaT cells were infected with 100 μ L of the viral inoculum for 1 hour at 37°C and 5% CO₂ with rocking. After the 1-hour infection, the inoculum was removed and the cells were supplemented with new DMEM10.

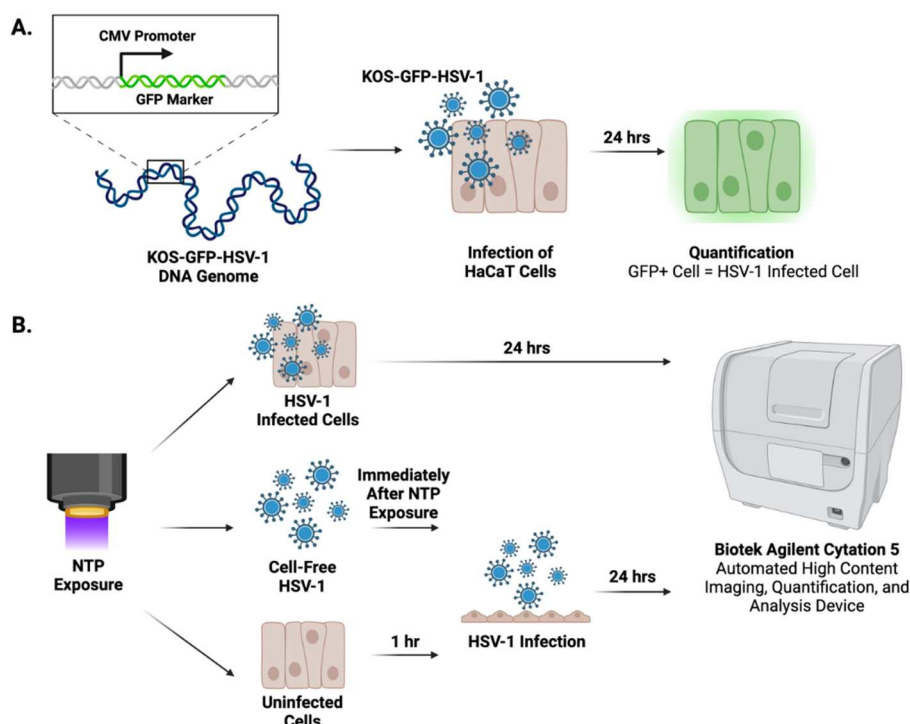


Figure 1. Experimental Design. (A) A KOS-GFP-HSV-1 strain was used to infect HaCaT cells. HSV-1-infected cells were quantified 24 hours post-infection by GFP expression. (B) Overview of the in vitro model for treating cold sores with NTP. Cell-free HSV-1, HSV-1-infected cells, or uninfected cells were exposed to NTP. The antiviral effects were assessed in situ at 24 hours post infection on an automated Agilent Biotek Cytation 5 high content imaging system.

2.3. NTP devices

A FE-DBD 12-well electrode connected to an electrical power supply was used to investigate the antiviral activity of NTP on HSV-1 infection. The 12-well electrode consists of a copper electrode surrounded by quartz dielectric material casing. A Z-positioner was used to set the distance of the electrode to 1 mm from the bottom of the 12-well plate placed on a metal ground plate (Figure 2A). The voltage, frequency, and exposure time were set on the power supply.

For comparison, a 2D-DBD device (described in detail in [18]) was used. The electrode consists of a 2D-array of micro-discharges encased in a polytetrafluoroethylene electrode holder that facilitates the continuous flow of ambient air at a rate of 15 slm (standard liter per minute). The electrode was driven by an AC power supply at a frequency of 30 kHz. The applied voltage amplitude was monitored with a high voltage probe through an oscilloscope and kept at 5 kV corresponding to an average power of ~ 5 W. The distance between the 2D-DBD array and the sample was controlled using an adjustable platform (Figure 2B). The electrode was centered over a 3 \times 3 grid of wells in a 96-well plate, resulting in simultaneous exposure of all nine wells in the grid to the NTP airflow.

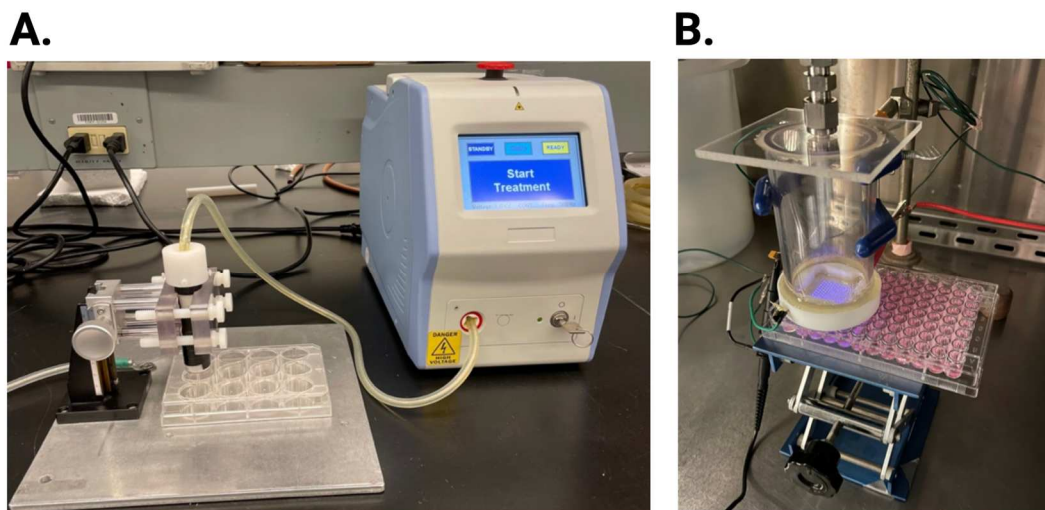


Figure 2. NTP devices. NTP was generated using a FE-DBD electrode (A) or a 2D-DBD electrode with a continuous air flow (B). In each device configuration, the distance from the electrode to the bottom of the plate was controlled mechanically.

2.4. Application of NTP

For NTP application using the FE-DBD, HaCaT cells were seeded at 6×10^5 cells/mL in 1 mL of DMEM10 into each well of a 12-well plate. Cells were grown to confluence over a 24- to 26-hour period. The cells were washed with PBS and then the 12-well plate was fitted with a metal grounding plate. Following removal of the PBS from the cells, the electrode was placed 1 mm above the bottom of each well using an electrode holder with an XY positioner. NTP was applied to HaCaT cells for 20 seconds at 8.5 kV and 400 Hz frequency. Immediately after NTP exposure, cells were supplemented with 1 mL of DMEM and incubated at 37°C and 5% CO₂ for 24 hours. For HSV-1-infected cells, NTP exposure took place immediately after the 1-hour HSV-1 infection period. Uninfected HaCaT cells were exposed to NTP and infected with HSV-1 after 1 hour of incubation.

For exposure of cell-free HSV-1 to FE-DBD, a viral inoculum at a concentration of 6×10^6 PFU/mL was prepared in 1 mL of serum-free DMEM. NTP was applied to 400 μ L of this inoculum in a well of the 12-well plate at a distance of 2 mm from the bottom of the well for 20 seconds at 8.5 kV and frequencies of 400 Hz, 500 Hz, and 1000 Hz. Immediately after NTP exposure, 100 μ L of the viral inoculum (MOI 1) was added to confluent HaCaT cells in a 12-well plate (plated at 6×10^5 cells per well). After allowing infection to proceed for 1 hour, the inoculum was removed and cells were supplemented with 1 mL new DMEM10 and incubated at 37°C and 5% CO₂ for 24 hours.

For the 2D-DBD device, HaCaT cells were seeded in 96-well plates at a seeding density of 7×10^4 cells/well in 100 μ L DMEM10 and grown to confluence over a 24- to 26-hour period. Prior to NTP exposure, cells were washed with PBS and 100 μ L of fresh DMEM10 was added to each well. The base of the electrode housing was lowered to touch the top of the 96-well plate. This resulted in a distance of approximately 14 mm between the electrode array and the bottom of the well. HaCaT cells in DMEM10 were exposed to NTP for 7 minutes. For HSV-1-infected cells, NTP exposure took place immediately after the 1-hour HSV-1 infection period. One-hour post-NTP exposure, the media was replaced with new DMEM10 (not exposed to NTP). Uninfected HaCaT cells were exposed to NTP and infected with HSV-1 after 1 hour of incubation.

In experiments involving application of 2D-DBD plasma to cell-free HSV-1, the virus was suspended in serum-free DMEM at a concentration of 7×10^5 PFU/mL and exposed to NTP for 4, 5, 6, or 7 minutes in a 6-well plate. Immediately after NTP exposure, 100 μ L of the viral inoculum (MOI 1) was added to confluent HaCaT cells in a 96-well plate. After a 1-hour infection incubation, the inoculum was removed and cells were supplemented with 100 μ L DMEM10 and incubated at 37°C and 5% CO₂ for 24 hours.

The experiments involving NTP and infectious material were conducted as approved by the Drexel University Institutional Biosafety Committee in Biosafety Level 2 biosafety cabinet.

2.5. Quantification of HSV-1-infected cells

A recombinant strain of HSV-1 (KOS-GFP-HSV-1) was used for all experiments. This strain facilitated the detection of infected cells via GFP reporter expression (Figure 1A). At 24 hours post-infection, the Cytation 5 was used to image and quantify GFP expressing cells (Figure 1B). Image analysis was performed using the Gen5 program (version 3.11) (Agilent Technologies, Santa Clara, CA). Images were acquired using a 4x magnification lens with the brightfield high contrast and GFP channels. Total cells, GFP+ cells, and the mean fluorescent intensity (MFI) of each well were quantified from images captured at 4x magnification by the Cytation 5. The percentage of GFP+ cells was calculated by dividing the number of GFP+ cells by the total cell count for each image.

2.6. Determination of HaCaT cell viability

Twenty-four hours post-exposure to NTP, cells were stained with 1 $\mu\text{g}/\mu\text{L}$ propidium iodide (PI). Detection and quantification of PI-positive cells were accomplished using the Cytation 5. Image analysis was performed using the Gen5 program. Images were taken at 4x magnification and the PI channel was used to measure fluorescence. The number of PI-positive cells and total number of cells in each well were used to calculate percent viability. Viability calculations were normalized to those of uninfected HaCaT cells not exposed to NTP.

2.7. Quantification of hydrogen peroxide and nitrite

To determine concentrations of hydrogen peroxide and nitrite after NTP application, phenol red-free DMEM10 (used to avoid interference with absorbance readings) was exposed to NTP in the absence of cells or in the presence of HaCaT cells plated at the same seeding densities used in the protocol for each device.

NTP exposure procedures were device dependent. For the FE-DBD, 100 μL of phenol red-free DMEM was aliquoted into each well of a 12-well plate, exposed to NTP at 400, 500, and 1000 Hz, and supplemented with 900 μL of phenol red-free DMEM immediately after exposure. For the 2D-DBD, 100 μL of phenol red-free DMEM was added to every well in each 96-well plate. NTP exposure was conducted by centering the 2D-DBD electrode housing over a 3x3 grid of nine wells. Immediately after NTP exposure, the medium was transferred to the assay plate.

The Spectroquant hydrogen peroxide test procedure (Millipore Sigma; Cat. 118789) and the Invitrogen Griess Reagent procedure (Invitrogen; Cat. G7921) were used for the quantification of hydrogen peroxide and nitrite, respectively. All quantification assays were performed as described by the manufacturer. Absorbance was read using the Cytation 5 and the data were exported to an Excel file. Based on the respective line equation calculated from the standard curve, absorbance readings were used to determine the concentrations of hydrogen peroxide and nitrite in μM . To account for kit error, the concentration values of the NTP-exposed samples were subtracted by the concentration values of their respective No NTP control [28].

2.8. Statistical Analysis

A one-way ANOVA was performed for the analysis of cell-free HSV-1 studies. All other experiments were analyzed using a two-way ANOVA to determine statistical significance. Statistics were deemed significant if $p < 0.05$. All data were plotted and analyzed using GraphPad Prism version 9.5 (GraphPad Software, Boston, MA).

3. Results

3.1. NTP exposure reduces the infectivity of cell-free HSV-1

NTP devices can be used to produce antiviral effects against many viruses [16,18,29]. To investigate the effects of FE-DBD and 2D-DBD on HSV-1 infectivity, we established operating conditions to deliver NTP to cell-free virus suspensions (Figure 3A). The FE-DBD plasma reduced infectivity of cell-free HSV-1 in a frequency-dependent manner to 89% at 400 Hz and a statistically significant 70% at the highest frequency (1000 Hz) (Figure 3B). Mean fluorescent intensity (MFI), which is an indicator of viral gene expression levels, decreased with increasing NTP frequency from 86% at 400 Hz to 66% at 1000 Hz (relative to the infected control) (Figure 3C). A similar dose-dependent trend toward reduced viral infectivity was observed after exposure to 2D-DBD plasma

(89% infectivity after a 4 minute exposure and a reduction to 63% at 7 minutes) (Figure 3D). Similarly, MFI trended down with increased exposure time (80% at 4 minutes to 66% at 7 minutes, relative to the infected cell control) (Figure 3E). These results demonstrated that NTP negatively impacted the ability of HSV-1 to infect target cells. While this antiviral effect is likely attributable to interference with an aspect of virus binding and entry, NTP dose-dependent reductions in MFI also suggest that NTP affects viral gene expression subsequent to entry into the host cell.

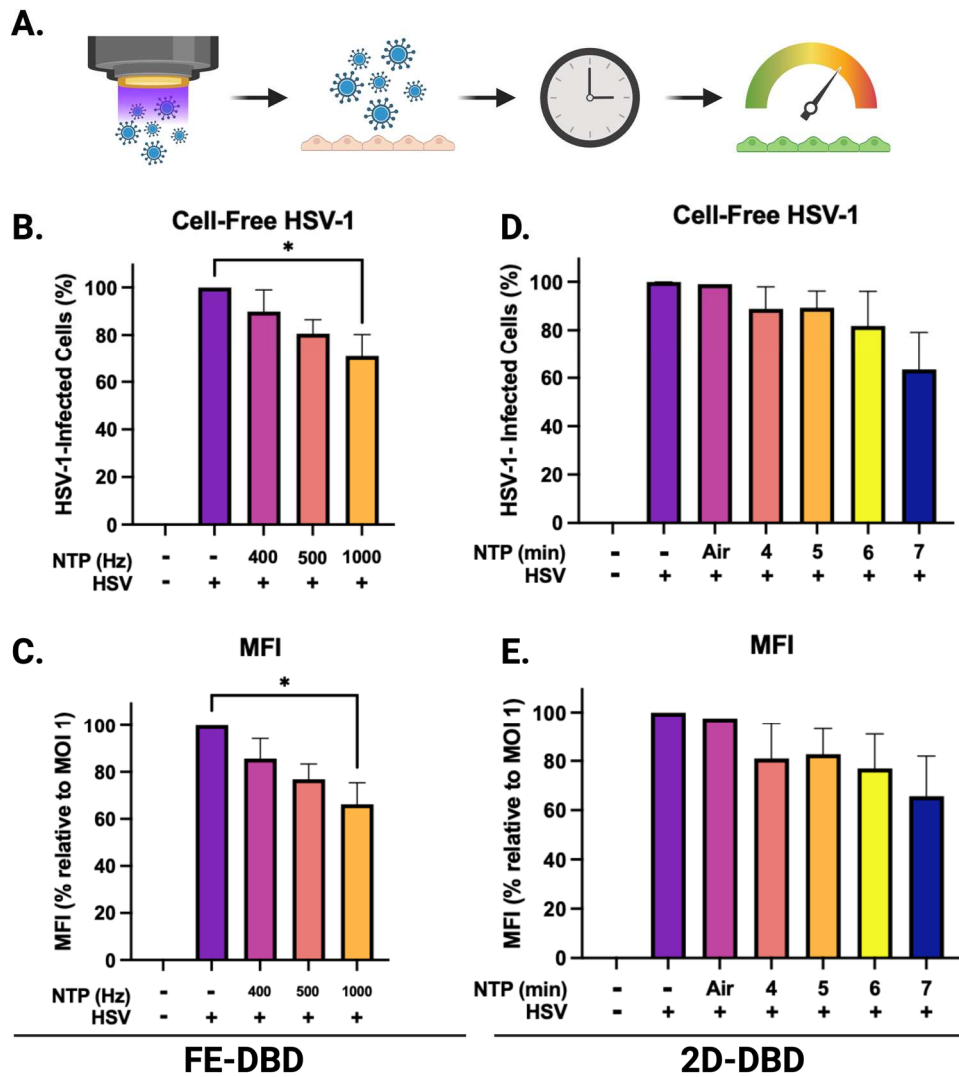


Figure 3. FE-DBD and 2D-DBD reduced HSV-1 infectivity and gene expression in cells. (A) Schematic of experimental timeline: Preparations of cell-free HSV-1 in media were exposed to NTP and then used to infect HaCaT cells immediately after NTP exposure. GFP expression was measured 24 hours post-infection. (B) and (C) show the frequency-dependent decreases in the percent infected cells and decreases in MFI after infection with FE-DBD-exposed cell-free HSV-1. (D) and (E) Exposure duration-dependent trends toward reduced infectivity and MFI were observed after 2D-DBD plasma application to cell-free HSV-1. * $p < 0.05$.

3.2. NTP disrupts viral replication and gene expression in HSV-1-infected HaCaT cells

While the antiviral effect of NTP on cell-free viruses has been shown [16,18], few studies have investigated the impact of NTP on productive viral infection in cells [22,30]. To examine this effect, HSV-1-infected HaCaT cells were subjected to NTP application after infection (Figure 4A). Three MOIs were used for the infection of HaCaT cells to determine the effectiveness of NTP against virus replication.

We elected to expose infected cells to FE-DBD at a frequency of 400 Hz because the viability of uninfected cells was unaffected by NTP exposure at this frequency (Figure 4B). At 0.5 MOI, the number of HSV-1-infected cells was significantly reduced by post-infection NTP application (~70% reduction relative to cells infected without subsequent NTP application). At 0.1 MOI, post-infection NTP application appeared to reduce the number of HSV-1-infected cells to an even greater extent (>70% reduction relative to control cells). However, this reduction was not statistically significant likely due to low numbers of infected cells at that MOI. When cells were infected at the highest virus inoculum (MOI 1), no significant changes in the number of infected cells were measured 24 hours post-NTP application (Figure 4C). As an additional indicator for NTP antiviral activity, MFI followed similar trends with a significant NTP-associated reduction measured at 0.5 MOI (Figure 4D). Our results suggest that NTP application can adversely affect HSV-1 replication post-entry. Since GFP expression is a measure of IE promoter activity, reductions in MFI suggest that inhibition of IE viral gene expression may be part of the mechanism of action of NTP.

A 7-minute NTP exposure was selected for application of 2D-DBD plasma to infected cells, since this exposure duration yielded no significant changes in viability of uninfected cells (Figure 4E). While similar trends of fewer infected cells (Figure 4F) and lower MFI (Figure 4G) in response to NTP were observed at each MOI, no statistically significant changes were measured.

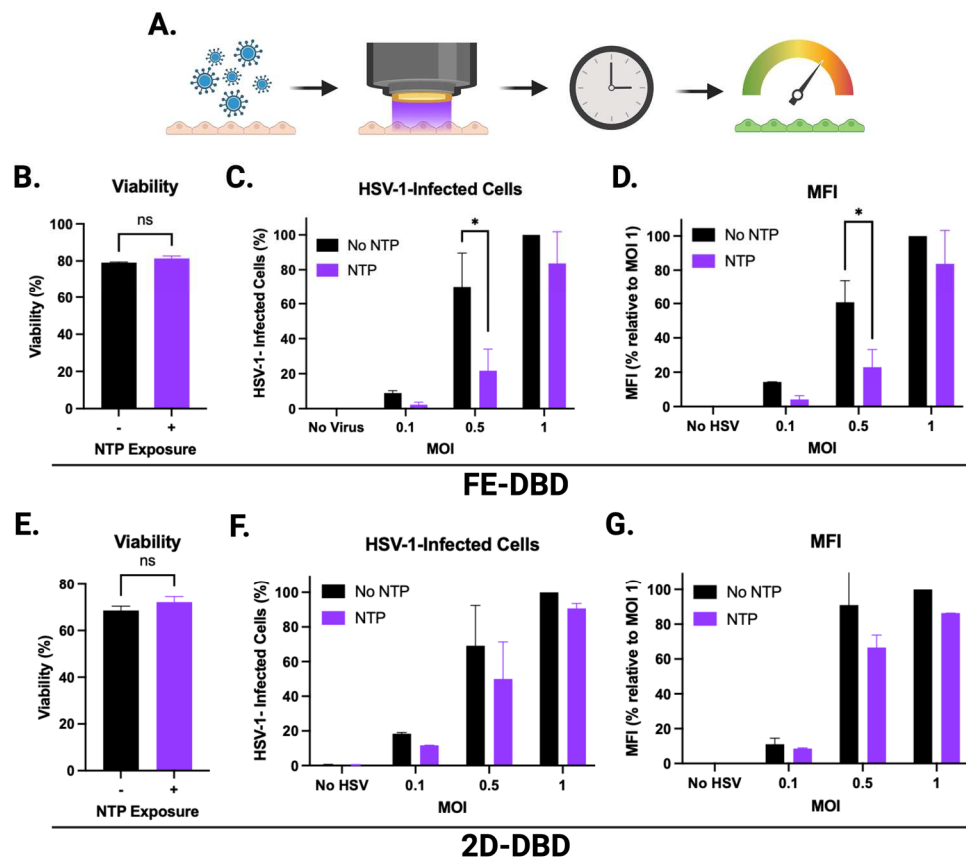


Figure 4. FE-DBD and 2D-DBD reduced numbers of HSV-1-infected cells 24 hours post-NTP exposure. (A) Schematic of experimental timeline: HSV-1-infected HaCaT cells were exposed to NTP and measured for GFP expression 24 hours later. (B) At 400 Hz, FE-DBD did not significantly impact viability of uninfected HaCaT cells. (C) Exposure of HSV-1-infected HaCaT cells to NTP at 400 Hz produced by FE-DBD resulted in a reduced numbers of infected cells 24 hours post-infection. Infected cells were quantified by GFP expression. (D) FE-DBD also decreased the MFI of cells infected with HSV-1 24 hours post-NTP exposure. (E) At 7 minutes NTP exposure using 2D-DBD, there were no significant changes in HaCaT cell viability. (F) The 2D-DBD reduced the number of infected cells and the MFI within cells 24 hours after their exposure to NTP (G) but this reduction was not statistically significant. Percent infected cells in (C) and (F) were calculated relative to the number of HSV-1-infected cells detected after infection at 1 MOI without subsequent NTP application. * $p < 0.05$.

3.3. NTP exposure impacts the susceptibility of HaCaT cells to infection with HSV-1

Newly released HSV-1 virions spread from a productively infected cell to neighboring uninfected cells by diffusion through the extracellular space or by spreading cell to cell via cellular junctions [31]. As targets in cold sores, uninfected epithelial cells that are rendered less susceptible to HSV-1 by NTP treatment could be an important aspect of reducing the local spread of HSV-1 within the lesion, hastening virus clearance, and lesion resolution. To examine the ability of NTP to reduce the susceptibility of cells to infection, uninfected cells were exposed to NTP at the selected doses and then infected 1 hour later with HSV-1 at three MOIs.

When uninfected HaCaT cells were exposed to FE-DBD, the number of infected cells was reduced by >70% during subsequent infections at 0.1 and 0.5 MOI relative to their respective controls. The reduction at 0.5 MOI was statistically significant while the observed reduction at 0.1 MOI was not. Additionally, the number of infected cells was significantly reduced (26% reduction) at 1.0 MOI (Figure 5B). These reductions suggest that NTP exposure inhibits infection of keratinocytes by HSV-1. MFI was decreased by ~70% at 0.5 MOI and 22% at 1 MOI with a reduction trend at MOI of 0.1 (Figure 5C). This result suggests that NTP-exposed cells, when subsequently infected, have reduced levels of IE viral gene expression as well as altered susceptibility to HSV-1 binding and/or entry. The result is consistent with observations made in experiments involving NTP application to cell-free HSV-1 (Figure 3). While the application of 2D-DBD resulted in similar trends toward reduced infection (Figure 5D) and apparently lower viral gene expression (Figure 5E), the effects of 2D-DBD were not statistically significant under the conditions of the experiments.

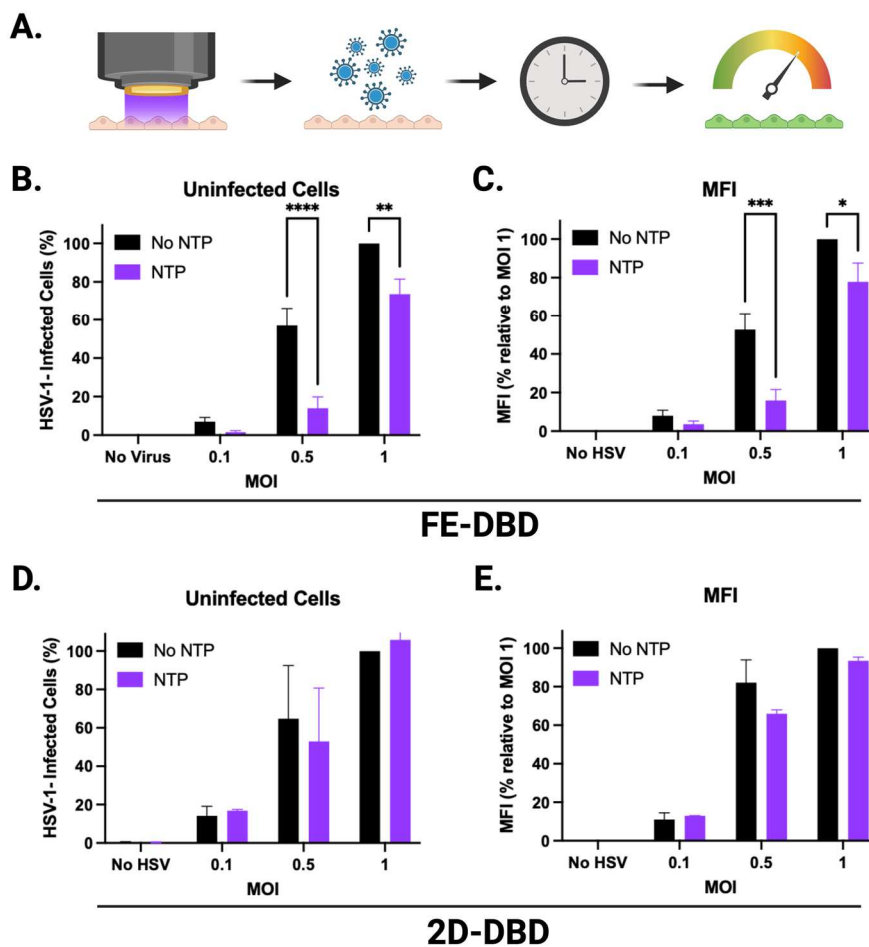


Figure 5. FE-DBD reduced the susceptibility of uninfected cells to infection with HSV-1. (A) Schematic of experimental timeline: Uninfected HaCaT cells were exposed to NTP and then infected with HSV-1 1 hour later. GFP expression was measured 24 hours later. (B) NTP exposure of uninfected cells to FE-DBD plasma reduced infection by HSV-1 1-hour post-exposure at three MOIs. (C) NTP exposure of uninfected cells also reduced levels of HSV-1 viral gene expression subsequent to infection. (D) 2D-

DBD had no significant impact on susceptibility of cells to HSV-1 infection or (E) in MFI measured 24 hours post-infection. Percent infected cells in (B) and (D) were calculated relative to the number of HSV-1-infected cells detected after infection at 1 MOI without pre-exposure to NTP. **** $p < 0.0001$, ** $p < 0.01$, * $p < 0.05$.

3.4. NTP produces long-lived RONS in media during exposure

To establish possible relationships between the observed antiviral effects of NTP and the RONS generated by NTP, two long-lived RONS – hydrogen peroxide and nitrite – were measured in cell culture medium with and without HaCaT cells subsequent to NTP exposure. Hydrogen peroxide and nitrite concentrations were measured immediately after NTP exposure and 24 hours post-NTP exposure to establish correlations with antiviral effects observed at 24 hours. Target cells (HaCaT keratinocytes) were introduced to investigate the contributions of cellular redox systems, which include enzymes and other molecules that produce or inactivate RONS to maintain cellular redox homeostasis [25,26], to changes in RONS concentrations.

In experiments involving FE-DBD plasma (Figure 6A-D), there was an overall increase in hydrogen peroxide immediately after NTP application at all frequencies tested relative to the no NTP controls, ranging from 38 μM to 50 μM (Figure 6A). These concentrations did not change significantly over 24 hours (Figure 6B). When HaCaT cells were introduced into the system, no apparent change in the concentration of hydrogen peroxide was observed at the 0 hour timepoint (Figure 6A). However, at 24 hours post-NTP exposure, hydrogen peroxide concentrations exceeded 200 μM in media containing HaCaT cells in all cases, even in cells not exposed to NTP. This suggests that the cells themselves produce considerable quantities of hydrogen peroxide over time independent of NTP (Figure 6B).

In contrast to FE-DBD, the concentrations of hydrogen peroxide in media alone were higher when the 2D-DBD was applied, ranging from 140 μM to 600 μM in an exposure duration-dependent manner and reduced by over 50% 24 hours later. In the presence of HaCaT cells, hydrogen peroxide concentrations were observably lower than in media alone at 400 and 1000 Hz (>40% reduction) (Figure 6E). While the no NTP cell control had 30 μM hydrogen peroxide after 24 hours incubation, samples exposed to NTP ranged from 240 μM to 270 μM . However, no exposure duration-dependent trend was observed (Figure 6F).

Nitrite concentrations immediately after FE-DBD NTP application were frequency-dependent and ranged in concentration from 9 μM to 17 μM . When HaCaT cells were present, nitrite concentrations decreased by a statistically significant ~40% for all groups (Figure 6C). After 24 hours, nitrite concentrations ranged from 7 μM to 20 μM with no statistical significance between groups (Figure 6D). While nitrite and reactive nitrogen intermediates have documented antimicrobial activities, this effect is pH-dependent [32]. Our previous studies have shown that the FE-DBD NTP application does not change the pH of media [25].

2D-DBD plasma also produced higher concentrations of nitrite (> 50 μM) compared to FE-DBD at both time points. There was no dependence of nitrite concentrations on exposure duration immediately after NTP exposure. Nitrite concentrations in the absence of cells ranged between 96 μM and 135 μM . When HaCaT cells were present, nitrite concentrations appeared to increase. However, the differences were not statistically significant (Figure 6G). After 24 hours, nitrite concentrations ranged from 82 μM to 102 μM in media with no trend in exposure duration. While the presence of HaCaT cells appeared to increase nitrite concentrations, this increase was only statistically significant at the 6-minute NTP exposure ($p = 0.0438$) (Figure 6H).

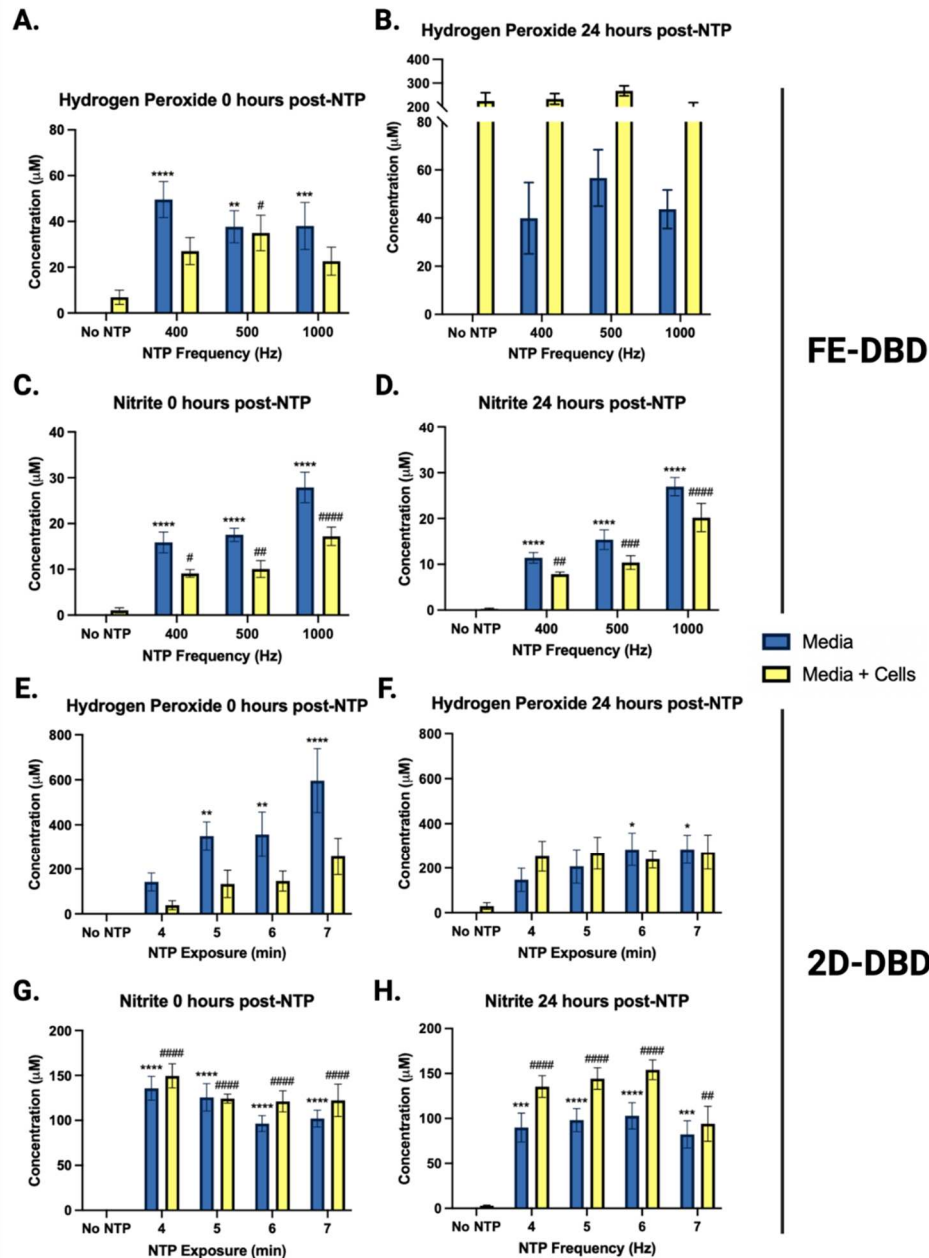


Figure 6. NTP increased hydrogen peroxide and nitrite concentrations in media. Hydrogen peroxide and nitrite concentrations were measured in media with and without HaCaT cells immediately after and 24 hours following exposure to NTP generated by (A-D) FE-DBD or (E-H) 2D-DBD. Statistical analyses were applied to comparisons of concentrations measured in media only with or without NTP application (denoted with one or more *) or concentrations measured in media with cells with or without NTP application (denoted with one or more #). ****/#### p < 0.0001, **/### p < 0.001, */## p < 0.01, */# p < 0.05.

4. Discussion

Herpes labialis is a lifelong disease with no available curative strategies, resulting in a large global health burden [5]. While nucleoside analogs, such as acyclovir, are effective in alleviating cold sores, they are unable to eliminate latent reservoirs that cause recurrent reactivation in patients [12,13]. This limitation, combined with emerging antiviral resistance [14], highlights a critical need for the development of new therapies that can suppress viral replication in cold sores while also reducing latent reservoirs in the TG and subsequent recurrences of clinical manifestations of HSV-1 reactivation.

Using our *in vitro* model of cold sore treatment with NTP, we investigated NTP as the basis of a therapy for *herpes labialis*. Our experiments demonstrated that the antiviral activities of NTP include (i) reductions in virus infectivity, (ii) reductions in cells infected with HSV-1, (iii) reductions in viral gene expression during replication in host cells, and (iv) reduced susceptibility of uninfected cells to HSV-1 infection. The first result was expected given previous demonstrations of the detrimental effects of NTP on cell-free virus. The second parallels and extends previous experimental results involving application of NTP to HSV-1-infected corneal epithelial cells [22]. However, the third and fourth activities are unique among published studies of the effects of NTP on viruses and viral infections.

Our experiments involving NTP application to HSV-1-infected cells demonstrated that NTP reduced the number of infected cells as well as levels of viral gene expression. However, our results also indicated that both effects were dependent on the magnitude of the infection (i.e., MOI). The greatest reductions in HSV-1-infected cells and MFI in response to NTP were observed at MOIs of 0.1 and 0.5. In contrast, the antiviral activities of NTP against cells infected at an MOI of 1 were negligible. The dependence of antiviral activity on MOI suggests that the availability of the NTP-associated factor responsible for the antiviral activity may be rate-limiting, as implied by the loss of activity in the presence of high percentage of HSV-1-infected cells. Although this result may inform an understanding of the mechanism(s) that underlie the antiviral activities, it does not diminish the potential of NTP as a therapy for HSV-1 infection since a condition equivalent to an MOI of 1 is unlikely in a lesion typical of *herpes labialis*.

The effect of NTP on viral gene expression suggests that NTP disrupts IE viral gene transcription. These viral genes are important for the production of viral proteins that downregulate cellular antiviral responses as well as viral gene expression cascades that promote the progression through the viral replication cycle. Disruption of IE gene expression can lead to reduced expression of early (E) genes and late (L) genes that encode protein products for viral replication and assembly, respectively [33]. Disrupting viral gene expression in the host cell will result in less virus production, fewer infected cells at the site of infection, and a lower virus titer in the lesion. By reducing lytic infection locally, NTP treatment can reduce the titer of HSV-1 available for infecting adjacent mucosal epithelial cells and, importantly, for establishing latent infection in sensory neurons. These effects will be verified in a murine model of HSV-1 oral infection and pathogenesis, in which quantitative polymerase chain reaction (qPCR) and viral plaque assays will be used to verify the effects of NTP on *in vivo* viral gene expression and virus production, respectively [2]. The murine model will also allow us to test the hypothesis that reduction in HSV-1 production minimizes the establishment of latent reservoirs in the TG and, therefore, reduces the likelihood and/or frequency of reactivation and recurrent outbreaks of cold sores over time [26].

We also observed a reduced susceptibility to HSV-1 in uninfected cells exposed to NTP. It is likely that reduced susceptibility of HaCaT cells to HSV-1 is due to oxidation of cell surface receptors involved in HSV-1 entry, such as heparan sulfate. A similar mechanism was implied in experiments involving NTP and HIV-1 infection. In those studies, NTP altered the expression of extracellular receptors involved in viral entry during *in vitro* infection of HIV-1 [20].

In a clinical setting in which NTP is used to treat a cold sore, multiple mechanisms of antiviral activity, as demonstrated in our studies, will combine to increase the efficacy of the treatment. First, reductions in infectivity of cell-free viruses within the lesion will be achieved by modifications of glycoproteins, found on the surface of HSV-1 viral particles, involved in entry into the host cell. Second, reductions in viral gene expression will be achieved in cells already infected at the time of treatment. Third, NTP will reduce the susceptibility to infection of cells not yet infected in the lesion. Collectively, these effects will serve to reduce the viral titer in the lesion, reduce the spread of the virus, and decrease the pathogenesis associated with infection.

Through the use of two different NTP devices, we demonstrated that the treatment modality determines the efficacy of NTP and may be attributed to the individual experimental setups required. The electrode used to generate FE-DBD was designed to fit inside a well in a 12-well plate (6x10⁵ cells/well) and deliver NTP at a distance of 1 mm from cells on the bottom surface of the well. In contrast, the 2D-DBD electrode rested on top of a 96-well plate where the cell density was 7x10⁴/well and the distance between the electrode and cells was ~14 mm. The disparity in numbers of cells

exposed to NTP for each device and the distance from the electrode may have contributed to some of the differences in our experimental observations.

Additional key differences between the two devices were the presence or absence of cell culture medium during NTP application to cells and the electrical characteristics of each device design. FE-DBD plasma was delivered after removal of medium from the well to allow a more “direct” application. During application of 2D-DBD plasma, the medium remained on the cells during NTP exposure to prevent cell loss due to dehydration during the extended exposures. Additionally, in the case of FE-DBD plasma, the target becomes part of the electrical circuit and is therefore exposed to short-lived metastable species, charged species, and electric fields [25]. In contrast, the 2D-DBD device mostly delivers NTP-exposed gas containing long-lived RONS to the target cells. In the 2D-DBD device design, the target cells are not part of electrical circuit through which the NTP is generated.

We also measured RONS produced by NTP generated by the two devices. The hypothesis driving our studies was that changes in hydrogen peroxide and nitrite concentrations correlate with NTP-associated antiviral activities demonstrated in experiments involving cell-free virus, infected cells, and uninfected cells. However, we were unable to validate this hypothesis to draw conclusions about the contributions of RONS to the demonstrated antiviral effects of NTP.

RONS are proposed to be the dominant effectors in NTP’s antiviral effects. 2D-DBD, previously shown to have antiviral activity against cell-free FCV [18], is characterized by the generation of long-lived RONS. A 7-minute 2D-DBD NTP exposure, which was applied to HSV-1-infected and uninfected cells, produced ~596 μM hydrogen peroxide and ~102 μM nitrite in media. Under these treatment conditions, the 2D-DBD did not significantly reduce HSV-1 replication in infected cells or the susceptibility of uninfected cells to HSV-1. At 400 Hz (50 μM hydrogen peroxide and 28 μM nitrite), FE-DBD NTP exhibited greater efficacy against HSV-1-infected cells and uninfected cells. Together, these observations suggest that long-lived RONS are not primarily responsible for NTP’s antiviral mechanism against HSV-1 infection. Other components, including short-lived RONS, charged species, or electric fields that do not reach the cells when the 2D-DBD NTP is delivered, may contribute to the efficacy of NTP. Under our experimental conditions, the antiviral effectiveness was device dependent.

Overall, these initial studies provide the first insights into a potential NTP-based therapy against oral HSV-1 infection. We show that NTP reduced cell-free HSV-1 infectivity, diminished viral gene expression, and reduced the susceptibility of uninfected cells to HSV-1. Based on these results, we conclude that the combined antiviral effects of NTP could lead to reduced spread of HSV-1 to nearby cells in an infected lesion as well as to the TG where the virus establishes latent infection. This would reduce the frequency of viral reactivation and therefore in cold sore outbreaks.

We will validate this hypothesis *in vivo* using a mouse model that can replicate cold sore formation using the lip scarification method of infection [2]. This model will allow us to examine the resolution of cold sores and the impact of NTP on lesion resolution, virus titer in the lesion, and the establishment of latency in innervating nerves. In addition, the mouse model of NTP treatment for oral HSV-1 infection will facilitate investigations of the immunomodulatory impact of NTP on HSV-1 infection, spread, and clearance. NTP can stimulate the local release of immunogenic molecules from exposed cells as well as innate immune responses in exposed cells. We have previously demonstrated this effect in a lymphocyte cell line that models latent HIV-1 infection [30] and in mice bearing colorectal tumors [34]. The role of NTP-induced innate and adaptive immune responses in clearing acute HSV-1 infection and abating recurrent infections will be explored in this mouse model. Our initial investigations of the effect of NTP on early events in HSV-1 infection strongly suggest that NTP can serve as a therapeutic alternative that can address both lytic and latent infection, and will stimulate a specific anti-HSV-1 immune response that will extend the effectiveness of NTP treatment well beyond the short duration of the treatment.

5. Conclusion

We provide the first results of investigations into an NTP-based therapy for *herpes labialis* and the management of cold sore outbreaks. Our *in vitro* results imply that the antiviral effects of NTP applied to a herpetic lesion will reduce productive viral replication, limit the spread of HSV-1 to nearby cells, and alter the susceptibility of uninfected cells. Furthermore, our results suggest that the

antiviral effectiveness will be dependent on the NTP-generating device used for treatment and should be a factor in selecting the appropriate treatment modality for clinical use.

Author Contributions: Conceptualization, J.S., B.W., F.C.K., and V.M.; methodology, J.S., F.C.K., and V.M.; validation, J.S., P.J.B., B.W., F.C.K., and V.M.; formal analysis, J.S., J.B.; investigation, J.S.; resources, F.C.K. and V.M.; data curation, J.S.; writing—original draft preparation, J.S. and V.M.; writing—review and editing, J.S., B.W., P.J.B., F.C.K., and V.M.; visualization, J.S., B.W., F.C.K., and V.M.; supervision, F.C.K. and V.M.; project administration, F.C.K. and V.M.; funding acquisition, F.C.K. and V.M. All authors have read and agreed to the published version of the manuscript." Please turn to the CRediT taxonomy for the term explanation. Authorship must be limited to those who have contributed substantially to the work reported.

Funding: This research was partially supported by funds awarded to Vandana Miller, MD and Fred Krebs, PhD by the Drexel University Coulter Translational Research Award and the Institute for Molecular Medicine and Infections Disease. The work was also partially supported by a National Science Foundation Award PHY 2020695 to Peter Bruggeman, PhD.

Institutional Review Board Statement: Not applicable.

Informed Consent Statement: Not applicable.

Data Availability Statement: Relevant data are contained within the article.

Acknowledgments: We would like to acknowledge Gaurav Nayak for the 2D-DBD device set-up and training.

Conflicts of Interest: The authors declare no conflict of interest.

References

1. Whitley, R. and J. Baines, *Clinical management of herpes simplex virus infections: past, present, and future*. F1000Research, 2018. 7: p. 1726.
2. Egan, K.P., A.G. Allen, B. Wigdahl, and S.R. Jennings, *Modeling the pathology, immune responses, and kinetics of HSV-1 replication in the lip scarification model*. *Virology*, 2018. **514**: p. 124-133.
3. Harkness, J.M., M. Kader, and N.A. DeLuca, *Transcription of the herpes simplex virus 1 genome during productive and quiescent infection of neuronal and nonneuronal cells*. *Journal of virology*, 2014. **88**(12): p. 6847-6861.
4. Nicoll, M.P., W. Hann, M. Shivkumar, L.E.R. Harman, V. Connor, H.M. Coleman, J.T. Proença, and S. Efstathiou, *The HSV-1 Latency-Associated Transcript Functions to Repress Latent Phase Lytic Gene Expression and Suppress Virus Reactivation from Latently Infected Neurons*. *PLoS pathogens*, 2016. **12**(4): p. e1005539-e1005539.
5. *Herpes Simplex Virus*. 2022 12/16/22]; Available from: <https://www.who.int/news-room/fact-sheets/detail/herpes-simplex-virus>.
6. Bradshaw, M.J. and A. Venkatesan, *Herpes Simplex Virus-1 Encephalitis in Adults: Pathophysiology, Diagnosis, and Management*. *Neurotherapeutics : the journal of the American Society for Experimental NeuroTherapeutics*, 2016. **13**(3): p. 493-508.
7. Shah, A., A.V. Farooq, V. Tiwari, M.-J. Kim, and D. Shukla, *HSV-1 infection of human corneal epithelial cells: receptor-mediated entry and trends of re-infection*. *Molecular vision*, 2010. **16**: p. 2476-2486.
8. Cairns Dana, M., N. Rouleau, N. Parker Rachael, G. Walsh Katherine, L. Gehrke, and L. Kaplan David, *A 3D human brain-like tissue model of herpes-induced Alzheimer's disease*. *Science Advances*. **6**(19): p. eaay8828.
9. Itzhaki, R.F., *Herpes simplex virus type 1 and Alzheimer's disease: increasing evidence for a major role of the virus*. *Frontiers in aging neuroscience*, 2014. **6**: p. 202-202.
10. Santana, S., I. Sastre, M. Recuero, M.J. Bullido, and J. Aldudo, *Oxidative Stress Enhances Neurodegeneration Markers Induced by Herpes Simplex Virus Type 1 Infection in Human Neuroblastoma Cells*. *PLOS ONE*, 2013. **8**(10): p. e75842.
11. Vaghela, D., E. Davies, G. Murray, C. Convery, and L. Walker, *Guideline for the Management Herpes Simplex 1 and Cosmetic Interventions*. *The Journal of clinical and aesthetic dermatology*, 2021. **14**(6 Suppl 1): p. S11-S14.
12. Cernik, C., K. Gallina, and R.T. Brodell, *The Treatment of Herpes Simplex Infections: An Evidence-Based Review*. *Archives of Internal Medicine*, 2008. **168**(11): p. 1137-1144.
13. Ibáñez, F.J., M.A. Fariás, M.P. Gonzalez-Troncoso, N. Corrales, L.F. Duarte, A. Retamal-Díaz, and P.A. González, *Experimental Dissection of the Lytic Replication Cycles of Herpes Simplex Viruses in vitro*. *Frontiers in microbiology*, 2018. **9**: p. 2406-2406.
14. Bacon, T.H., M.J. Levin, J.J. Leary, R.T. Sarisky, and D. Sutton, *Herpes simplex virus resistance to acyclovir and penciclovir after two decades of antiviral therapy*. *Clinical microbiology reviews*, 2003. **16**(1): p. 114-128.

15. von Woedtke, T., A. Schmidt, S. Bekeschus, K. Wende, and K.D. Weltmann, *Plasma Medicine: A Field of Applied Redox Biology*. In Vivo, 2019. **33**(4): p. 1011-1026.
16. Mohamed, H., G. Nayak, N. Rendine, B. Wigdahl, F.C. Krebs, P.J. Bruggeman, and V. Miller, *Non-Thermal Plasma as a Novel Strategy for Treating or Preventing Viral Infection and Associated Disease*. Frontiers in Physics, 2021. **9**: p. 286.
17. Aboubakr, H.A., P. Williams, U. Gangal, M.M. Youssef, S.A.A. El-Sohaimy, P.J. Bruggeman, and S.M. Goyal, *Virucidal effect of cold atmospheric gaseous plasma on feline calicivirus, a surrogate for human norovirus*. Applied and environmental microbiology, 2015. **81**(11): p. 3612-3622.
18. Nayak, G., H.A. Aboubakr, S.M. Goyal, and P.J. Bruggeman, *Reactive species responsible for the inactivation of feline calicivirus by a two-dimensional array of integrated coaxial microhollow dielectric barrier discharges in air*. Plasma Processes and Polymers, 2018. **15**(1): p. 1700119.
19. Shi, X., G. Zhang, X. Wu, Z. Peng, Z. Zhang, X. Shao, and Z. Chang, *Effect of Low-Temperature Plasma on Deactivation of Hepatitis B Virus*. IEEE Transactions on Plasma Science, 2012. **40**(10): p. 2711-2716.
20. Volotskova, O., L. Dubrovsky, M. Keidar, and M. Bukrinsky, *Cold Atmospheric Plasma Inhibits HIV-1 Replication in Macrophages by Targeting Both the Virus and the Cells*. PloS one, 2016. **11**(10): p. e0165322-e0165322.
21. Jin, T., Y. Xu, C. Dai, X. Zhou, Q. Xu, and Z. Wu, *Cold atmospheric plasma: A non-negligible strategy for viral RNA inactivation to prevent SARS-CoV-2 environmental transmission*. AIP Advances, 2021. **11**(8): p. 085019.
22. Alekseev, O., K. Donovan, V. Limonnik, and J. Azizkhan-Clifford, *Nonthermal Dielectric Barrier Discharge (DBD) Plasma Suppresses Herpes Simplex Virus Type 1 (HSV-1) Replication in Corneal Epithelium*. Transl Vis Sci Technol, 2014. **3**(2): p. 2.
23. Brun, P., P. Brun, M. Vono, P. Venier, E. Tarricone, V. Deligianni, E. Martines, M. Zuin, S. Spagnolo, R. Cavazzana, R. Cardin, I. Castagliuolo, A.L.G. Valerio, and A. Leonardi, *Disinfection of ocular cells and tissues by atmospheric-pressure cold plasma*. PloS one, 2012. **7**(3): p. e33245-e33245.
24. Alekseev, O., W.E. Donegan, K.R. Donovan, V. Limonnik, and J. Azizkhan-Clifford, *HSV-1 Hijacks the Host DNA Damage Response in Corneal Epithelial Cells through ICP4-Mediated Activation of ATM*. Investigative Ophthalmology & Visual Science, 2020. **61**(6): p. 39-39.
25. Sutter, J., J. Bretschneider, S. Mamchur, F. Krebs, S. Gershman, and V. Miller *Inclusion of Biological Targets in the Analysis of Electrical Characteristics of Non-Thermal Plasma Discharge*. Plasma, 2023. **6**, 577-591 DOI: 10.3390/plasma6030040.
26. Sutter, J., P.J. Bruggeman, B. Wigdahl, F.C. Krebs, and V. Miller, *Manipulation of Oxidative Stress Responses by Non-Thermal Plasma to Treat Herpes Simplex Virus Type 1 Infection and Disease*. International journal of molecular sciences, 2023. **24**(5): p. 4673.
27. Boukamp, P., R.T. Petrussevska, D. Breitkreutz, J. Hornung, A. Markham, and N.E. Fusenig, *Normal keratinization in a spontaneously immortalized aneuploid human keratinocyte cell line*. Journal of Cell Biology, 1988. **106**(3): p. 761-771.
28. Veronico, V., P. Favia, F. Fracassi, R. Gristina, and E. Sardella, *Validation of colorimetric assays for hydrogen peroxide, nitrate and nitrite ions in complex plasma-treated water solutions*. Plasma Processes and Polymers, 2021. **18**(10): p. 2100062.
29. Nayak, G., A.J. Andrews, I. Marabella, H.A. Aboubakr, S.M. Goyal, B.A. Olson, M. Torremorell, and P.J. Bruggeman, *Rapid inactivation of airborne porcine reproductive and respiratory syndrome virus using an atmospheric pressure air plasma*. Plasma Processes and Polymers, 2020. **17**(10): p. 1900269.
30. Mohamed, H., R. Clemen, E. Freund, J.-W. Lackmann, K. Wende, J. Connors, E.K. Haddad, W. Dampier, B. Wigdahl, V. Miller, S. Bekeschus, and F.C. Krebs, *Non-thermal plasma modulates cellular markers associated with immunogenicity in a model of latent HIV-1 infection*. PLOS ONE, 2021. **16**(3): p. e0247125.
31. Rice, S.A., *Release of HSV-1 Cell-Free Virions: Mechanisms, Regulation, and Likely Role in Human-Human Transmission*. Viruses, 2021. **13**(12): p. 2395.
32. Klebanoff, S.J., *Reactive nitrogen intermediates and antimicrobial activity: role of nitrite*. Free Radic Biol Med, 1993. **14**(4): p. 351-360.
33. Kukhanova, M.K., A.N. Korovina, and S.N. Kochetkov, *Human herpes simplex virus: Life cycle and development of inhibitors*. Biochemistry (Moscow), 2014. **79**(13): p. 1635-1652.
34. Lin, A.G., B. Xiang, D.J. Merlino, T.R. Baybutt, J. Sahu, A. Fridman, A.E. Snook, and V. Miller, *Non-thermal plasma induces immunogenic cell death in vivo in murine CT26 colorectal tumors*. OncoImmunology, 2018. **7**(9): p. e1484978.

Disclaimer/Publisher's Note: The statements, opinions and data contained in all publications are solely those of the individual author(s) and contributor(s) and not of MDPI and/or the editor(s). MDPI and/or the editor(s) disclaim responsibility for any injury to people or property resulting from any ideas, methods, instructions or products referred to in the content.